

NASA Technical Paper 1323

NASA  
TP  
1323  
c.1

LOAN COPY: RET  
AFWL TECHNICAL  
KIRTLAND AFB,



# Ceramic Coating Effect on Liner Metal Temperatures of Film-Cooled Annular Combustor

Russell W. Claus, Jerrold D. Wear,  
and Curt H. Liebert

JANUARY 1979

**NASA**





NASA Technical Paper 1323

# Ceramic Coating Effect on Liner Metal Temperatures of Film-Cooled Annular Combustor

Russell W. Claus, Jerrold D. Wear,  
and Curt H. Liebert  
*Lewis Research Center  
Cleveland, Ohio*

**NASA**

National Aeronautics  
and Space Administration

**Scientific and Technical  
Information Office**

1979

## SUMMARY

An experimental and analytical investigation was conducted to determine the effect of a ceramic coating on the average metal temperatures of a full-annular, film-cooled combustion chamber liner. This investigation was conducted at pressures from 0.50 to 0.73 megapascal, inlet air temperatures of 589 and 894 K, and overall fuel-air ratios from 0.012 to 0.062. At all test conditions, experimental results indicate that application of a ceramic coating will result in significantly lower wall temperatures. At a fuel-air ratio of 0.06 with an inlet air temperature of 589 K (corresponding to an exhaust gas temperature of 2300 K), average coated-liner metal temperatures were 92 K lower than uncoated (bare) metal temperatures. In a simplified heat-transfer analysis, good agreement between experimental and calculated liner temperatures was achieved. Simulated spalling of a small portion of the ceramic coating resulted in only small increases in liner temperature because of the thermal conduction of heat from the hotter, uncoated area to the adjacent coated liner metal.

## INTRODUCTION

The current trend for advanced, fuel-efficient, commercial aircraft is toward turbofan engines with higher compressor pressure ratios and turbine inlet temperatures. This trend produces a more severe environment under which the entire combustion system, and in particular the combustor liner, must operate. The combustor liners of current high-performance engines generally use advanced film-cooling techniques or a combination of film and convection cooling. However, when pressure ratios and turbine inlet temperatures are increased for the next generation of turbofan engines, existing film-cooled-liner technology will probably not be sufficient to meet the demands placed upon it. Higher pressure ratios result in a greater radiative heat loading to the liner, a higher pressure differential across the liner, and lower film-cooling effectiveness due to the higher combustor inlet air temperatures. Higher turbine inlet temperatures result in a greater convective heat loading to the liner, and less available air for film cooling because near-stoichiometric burning must be maintained throughout the length of the combustor in order to reach the high turbine inlet temperatures.

A combustor liner cooling program is being pursued at the NASA Lewis Research Center to investigate various concepts, one of which is the use of ceramic thermal-barrier coatings. For these coatings to be useful in combustor liner applications, they

must result in substantially lower wall metal temperatures than bare-metal liners while withstanding thousands of hours of cyclic engine operation without cracking, spalling, or eroding. With the ceramic yttria-stabilized zirconia coating developed at Lewis (ref. 1), substantially lower turbine blade temperatures have been achieved (refs. 2 to 5). Furthermore, the coating withstood many hours of cyclic and steady-state high-temperature operation in good condition. The use of this coating on a single JT8D combustor liner is reported in reference 6. Substantial reductions in maximum liner temperatures were measured.

The present investigation was conducted to determine the effect of the yttria-stabilized zirconia coating on the average metal temperatures of a full-annular, film-cooled combustor liner. This liner was designed for operation with high inlet air temperatures and exhaust temperatures as high as 2300 K. Combustor inlet total pressure was varied from 0.50 to 0.73 megapascal at two inlet air temperatures, 589 and 894 K. A wide range of exhaust gas temperatures was obtained by taking data at fuel-air ratios of 0.012 to 0.062. Measured liner metal temperatures are compared with the results of a heat-transfer analysis that predicts liner metal temperatures, with and without ceramic thermal barriers, from combustor operating conditions. Coating durability was also monitored during the experiment.

## APPARATUS AND PROCEDURE

### Test Facility

The full-annular combustor tests were conducted in a duct test facility connected to a laboratory air supply and exhaust system. The facility capabilities are described in detail in reference 7. Airflow rates and combustor pressures were regulated by remotely controlled valves upstream and downstream of the test section. The airflow entering the combustor was evenly distributed by flow straighteners. For these tests, the airflow was heated to 589 and 894 K without vitiation before it entered the combustor.

### Research Combustor

Test rig. - Figure 1 is a schematic of the combustion test rig showing the airflow path through the rig, the combustor liner installation, the instrumentation planes, and various dimensions. The inlet centerbody contour increases the inlet airflow velocity to simulate the air discharge from an axial-flow compressor. The air then enters a dump diffuser, from which about 75 percent enters the air-blast fuel nozzles and the remainder flows along the inner and outer combustor annuli and through the film-cooling holes in the

combustor liner. There is no addition of dilution air to the combustion chamber. The combustion gases pass through an area that represents the turbine inlet area and are then cooled by water sprays before they enter a facility exhaust system. Fuel is introduced into the combustion system by two rows of 24 air-blast fuel nozzles. Fuel for each nozzle is supplied by a fuel tube (entering through the fuel plate) with a 0.098-centimeter-diameter discharge orifice. The fuel then impinges on a splash plate that shreds and atomizes the fuel.

Combustor liner installation. - The annular combustor liner used in these tests is shown in figure 2. An inner and outer liner form an annular combustion zone. Each liner is constructed of nine circumferential overlapping panels. Cooling air is directed onto the back side of a panel by a row of film-cooling air holes and is then discharged along the hot-gas side of the next downstream panel to form the cooling film. The combustor liner overall length is 23.9 centimeters, and the length from the air-blast fuel nozzle discharge plane to the exhaust instrumentation plane is 22.00 centimeters. The maximum cross-sectional area (reference area) of the combustor liner annulus is 0.2379 square meter. The panels were fabricated from Hastelloy X with a nominal thickness of 0.20 centimeter.

Instrumentation. - Inlet air instrumentation was mounted at planes 2 and 3, as shown in figure 1. There were eight equally spaced Chromel-Alumel thermocouples; eight total-pressure rakes of four probes each, installed at centers of equal areas; and 16 wall static-pressure taps, eight equally spaced around both the inner and outer diameter walls. The indicated readings of the inlet air thermocouples were taken as true values of the total temperature.

Exhaust gas instrumentation was mounted at plane 4. There were eight total-pressure rakes, five probes each, mounted at centers of equal areas. Static pressure was measured by four wedge static probes, equally spaced around the annulus at area centers. Average exhaust gas total temperatures were obtained from exhaust gas analysis. Four gas sample rakes, each with three area-centered probes, were equally spaced around the circumference.

Airflow rates were measured by a square-edged orifice installed according to ASME specifications. Fuel flowmeter rates were measured by turbine flowmeters with frequency-to-voltage converters for readout and recording. The fuel was ASTM Jet-A.

As shown in figure 2, 18 Chromel-Alumel thermocouples were installed on the hot-gas-side surface of panel 5 of both the inner and outer combustor liners. Thermocouples designated 1 to 9 were installed in the metal wall of the inner liner and thermocouples 10 to 18 were installed in the metal wall of the outer liner. All 18 thermocouples were used to evaluate the effect of the ceramic coating on liner metal temperatures in terms of average (arithmetical mean) and differential temperatures. The differential temperature was calculated by subtracting the inlet air temperature from the average liner metal temperature.

In addition to the 18 thermocouples on panel 5, one was mounted at bottom dead center on panel 3 of the outer diameter liner and was designated as thermocouple 19. All thermocouples were attached to the hot-gas side of the liner panels. Average liner temperature is determined from the thermocouples installed on panel 5.

### Liner Coating

The thermal-barrier-coated inner and outer liners are shown in figures 3 and 4. The procedure used for depositing the thermal-barrier coating onto the metal substrates of the liners was to prepare the substrate surface, arc-plasma spray on a layer of bond coating, and then arc-plasma spray on a layer of ceramic coating. The most current application process is described here.

Thermal-barrier coating application process. - Before coating, the bare metal surfaces were degreased and then grit blasted with commercial, pure (white) alumina. Using "white" alumina minimized the contamination that might occur with less-pure grit. The inlet supply pressure to the blasting equipment was 0.70 megapascal, and grit impingement was nearly normal to the surface. The alumina grit size was 250 micrometers, and the surface roughness after grit blasting was 6 micrometers (rms). Within 30 minutes after grit blasting, a bond coating of NiCrAlY (Ni-16Cr-6Al-0.5Y) was arc-plasma sprayed onto the grit-blasted surface to a thickness of  $0.010 \pm 0.005$  centimeter. The particle size of the bond powders fed into the arc-plasma spray gun was 44 to 74 micrometers. The measured roughness of the bond coating was 5 micrometers (rms). Within 30 minutes after bond-coating application, yttria-stabilized zirconia ceramic was applied to a thickness of  $0.050 \pm 0.008$  centimeter. The ceramic was hand smoothed with fine silicon carbide paper to a roughness of 1.5 to 3.0 micrometers (rms).

Coating equipment. - Commercial grit-blasting equipment was used to roughen the combustor metal surfaces. A hand-held arc-plasma spray gun was used to apply bond and ceramic powders. In the gun, an electric arc is contained within a water-cooled nozzle. Argon gas passes through the arc and is excited to temperatures of about 17 000 K. The bond and ceramic powders were mechanically fed into the nozzle and were almost instantaneously melted.

### Procedure and Test Conditions

The combustor liner coated with the ceramic as described in the previous section is shown in figure 3. The combustor was then tested at various operating conditions. After these tests the ceramic coating was removed from panel 5 - exposing the bare metal - and from around the thermocouple installed on panel 3, as shown in figure 4. The com-

bustor was then retested at the same operating conditions, which were as follows:

Combustor inlet total pressure, MPa . . . . .	0.50 - 0.73
Nominal combustor inlet air temperature, K . . . . .	589 and 894
Diffuser inlet Mach number . . . . .	0.286 - 0.415
Combustor average exhaust gas temperature, K . . . . .	1120 - 2380

## RESULTS AND DISCUSSION

The effect of the ceramic coating on the average combustor liner differential temperature at various fuel-air ratios is shown in figure 5. Liner differential temperatures were calculated by subtracting the inlet air temperature from the arithmetical average of all the panel 5 combustor liner thermocouple readings as previously noted in the section Instrumentation. The liner differential temperature at an inlet air temperature of 589 K (fig. 5(a)), linearly increases with fuel-air ratio. At an inlet air temperature of 894 K (fig. 5(b)), this same linear trend is exhibited to fuel-air ratios of about 0.06, where the slope of the liner differential temperature versus fuel-air ratio decreases. The addition of a ceramic coating gave lower panel 5 average and individual thermocouple readings at all fuel-air ratios investigated. At a fuel-air ratio of 0.06 and an inlet air temperature of 589 K (corresponding to an exhaust gas temperature of 2300 K), the maximum average liner temperature difference between the coated and uncoated liners was 92 K. At an inlet air temperature of 894 K, the difference between the coated- and the uncoated-liner average temperatures was about 20 K at a fuel-air ratio of 0.0175 and 70 K at a fuel-air ratio of 0.05. As would be expected, the maximum temperature reductions were observed at operating conditions where the heat flux to the liner wall was the largest. For the range examined, inlet air pressure had no discernible effect on liner temperature.

Figure 6, which shows the combined data of figures 5(a) and (b), demonstrates the similarity in differential liner temperature at the two inlet air temperatures. As the liner metal temperature is a direct function of the heat flux transmitted through the liner wall, the trend shown in figure 6 is indicative of relatively constant heat flux with respect to inlet air temperature. This conclusion is supported by the results of the heat-transfer analysis (appendix A).

During this investigation, no chipping or spalling of the ceramic coating was observed. Adherence of the coating was excellent. Warpage of a small section of the liner 3.2 centimeters by 2.5 centimeters and 0.3 centimeter deep caused by local metal over-temperature resulted in no damage to the ceramic coating. The combustor liner was subjected to several thermal cycles in which the fuel flow was immediately shut down while the combustor was operating at an exhaust gas temperature near 2300 K. This re-

sulted in a rapid cooling of the combustor liner with, again, no failure in the ceramic coating.

To simulate the effect of spalling of the ceramic coating, a small area of coating approximately 2 square centimeters in area was removed from around thermocouple 19 after it had been tested in a fully coated condition. (Thermocouple 19 was installed on panel 3.) The liner differential temperatures versus fuel-air ratio for thermocouple 19, both coated and uncoated, at an inlet air temperature of 894 K are shown in figure 7. The maximum temperature rise, due to removal of the ceramic coating, that was indicated by thermocouple 19 was approximately 24 K at a fuel-air ratio of about 0.03. By comparison, the average temperature rise that was indicated by the thermocouples on panel 5 at comparable conditions was 42 K. At other fuel-air ratios the temperature rise observed after removing the ceramic coating from the area around thermocouple 19 was even less significant. These readings indicate that there was significant thermal conductivity from the hotter, uncoated metal around thermocouple 19 to the cooler, coated metal just outside the uncoated area. This thermal conductivity kept the uncoated metal cooler than would occur if the whole panel or a large portion of the panel were uncoated. From these results it appears that spalling of the ceramic coating will increase metal temperatures only slightly, depending on the size of the spalled area and the thermal conductivity of the liner metal.

A heat-transfer analysis was made to determine if the liner metal temperature reductions possible through the use of ceramic coatings could be accurately predicted. The heat-transfer model used for these calculations is described in appendix A. Good agreement with the liner temperature reductions obtained with the ceramic coating were achieved when the absorptivity of the ceramic-coated wall was 0.5. With this wall absorptivity, the correction term suggested by McAdams was removed from the governing equation, as is more fully discussed in appendix A. A cold airflow calibration test of the combustor liner established that about 25 percent of the total airflow was used for liner cooling.

With this information, heat-transfer calculations were made for fuel-air ratios of 0.02, 0.03, 0.04, and 0.05 at the two inlet air temperatures that were tested experimentally. Figure 8 shows the liner differential temperature versus fuel-air ratio for both the experimentally determined and calculated liner average temperatures. To improve the agreement between experimental and calculated liner differential temperatures, the same method for determining the flame temperature was not used for all fuel-air ratios. This prevented the calculated liner differential temperatures from falling on a smooth curve as the experimental data did. It did, however, give good overall agreement between experimental and calculated liner differential temperatures. The poorest agreement was at a fuel-air ratio of 0.05 for both inlet air temperatures. At the 894 K inlet air temperature and 0.05 fuel-air ratio, the calculated bare-metal differential temperature was 29 K higher than the experimentally determined average. At the same fuel-

air ratio and an inlet air temperature of 589 K, the calculated bare-metal differential temperature was 27 K higher than the experimentally determined value. Calculations at the other fuel-air ratios all fell within  $\pm 15$  degrees Kelvin of the experimental values. This degree of computational accuracy indicates that liner metal temperature reductions available through the use of ceramic coatings can be accurately predicted by using the model detailed in appendix A.

## SUMMARY OF RESULTS

In investigating the effect that ceramic coating of the combustor liner had on liner metal temperatures, the following results were obtained:

1. Liner metal temperatures were substantially lower than those for same combustor with uncoated walls.
2. Calculated liner metal temperatures for both coated and uncoated walls were in general agreement with experimental results.
3. No cracking, spalling, or eroding of the ceramic coating was observed.
4. If a small portion of the ceramic coating should spall, thermal conduction from the hotter, uncoated liner metal to the cooler, coated liner metal will prevent large temperature increases in the bare-metal section.

Lewis Research Center,  
National Aeronautics and Space Administration,  
Cleveland, Ohio, Sept. 6, 1978,  
505-04.

## APPENDIX A

### HEAT-TRANSFER MODEL

The heat-transfer model closely follows the development detailed in references 8 and 9. The governing equation deals with steady-state heat transfer to a plate. Thermal conduction was considered both axially along the combustion chamber wall and radially through the wall. Axial thermal conduction was considered for the metal liner wall, and the axial conductivity of the ceramic was assumed to be negligible by comparison. Radial thermal conductivity of both the ceramic coating and the metal wall was introduced into the governing equation. A ceramic coating lowers liner temperatures in two ways: It acts as a thermal barrier to convective heat loadings because of its low thermal conductivity, and it reduces radiation heat loadings because its thermal absorptivity is lower than that of the bare metal. The governing equation is

$$R_1 + C_1 + (KC)_{\text{axial}} = (KC)_{\text{radial}} = R_2 + C_2 \quad (\text{A1})$$

This equation assumes that the axial, conductive heat-flux gradient is much smaller than the radial, conductive heat-flux gradient.

The radiant heat transfer from a graybody flame at temperature  $T_H$  to a blackbody wall at temperature  $T_{WH}$  is given by

$$R_1 = \sigma (\epsilon_H T_H^4 - \alpha_H T_{WH}^4) \quad (\text{A2})$$

To further simplify equation (A2) the following empirical formula by Lefebvre and Herbert was used:

$$\frac{\alpha_H}{\epsilon_H} = \left( \frac{T_H}{T_{WH}} \right)^{1.5} \quad (\text{A3})$$

Equation (A2) applies for radiation to a blackbody wall; but since the combustor liner is not a blackbody, reference 8 uses a correction term suggested by McAdams,  $1/2(1 + \alpha_W)$ . This correction term may be used for calculations involving a bare, oxidized liner panel wall that has an absorptance greater than 0.8 but should be disregarded for calculations involving ceramic-coated walls with much lower absorptances. Reference 10 shows that the absorptance of the ceramic thermal-barrier coating becomes much lower than 0.8 with increasing temperature. This is contrary to the behavior of bare, uncoated metals for which McAdams' correction factor is meant to apply. Therefore, applying the cor-

rection factor to calculations involving ceramic-coated liner walls would tend to over-estimate the radiation heat flux absorbed by the ceramic.

An absorptivity of 0.5 was used for calculations involving the ceramic thermal-barrier coating. Equation (A2) can then be written as

For uncoated liner walls:

$$R_1 = \sigma \left( \frac{1 + \alpha_W}{2} \right) \epsilon_H T_H^{1.5} (T_H^{2.5} - T_{WH}^{2.5}) \quad (A4)$$

For ceramic-coated liner walls:

$$R_1 = \sigma(0.5) \epsilon_H T_H^{1.5} (T_H^{2.5} - T_{WH}^{2.5}) \quad (A5)$$

The radiant heat transfer from the liner wall to the casing is given by

$$R_2 = \frac{\epsilon_W \epsilon_c}{\epsilon_c + \epsilon_W(1 - \epsilon_c)(A_W/A_c)} (T_{WA}^4 - T_c^4) \quad (A6)$$

The convective heat flux from the film-cooling air (hot-gas side) to the liner wall can be written as

$$C_1 = h_1 (T_f - T_{WH}) \quad (A7)$$

where

$$h_1 = 0.023 \frac{K_f}{D_{ft}} (Re)^{0.8} (Pr)^{0.4} \quad (A8)$$

with Re and Pr calculated at film conditions. The convective heat flux from the liner wall to the casing is determined by

$$C_2 = h_2 (T_{WA} - T_c) \quad (A9)$$

where

$$h_2 = 0.02 \frac{K_{an}}{D_{an}} (Re)_{an}^{0.8} (Pr)_{an}^{0.33} \quad (A10)$$

The radial heat flux conducted through the liner wall from the flame to the annulus air is

$$(KC)_{\text{radial}} = \frac{K_{\text{eff}}}{\delta_{\text{eff}}} (T_{\text{WH}} - T_{\text{WA}}) \quad (\text{A11})$$

$$\frac{K_{\text{eff}}}{\delta_{\text{eff}}} = \frac{1}{\frac{\delta_{\text{cerm}}}{K_{\text{cerm}}} + \frac{\delta_{\text{Hast}}}{K_{\text{Hast}}}} \quad (\text{A12})$$

For cases where the liner wall is uncoated,  $T_{\text{WH}} = T_{\text{WC}}$ . The axial conductive heat flux is approximated numerically by

$$(KC)_{\text{axial}} = K_{\text{Hast}} \delta_{\text{Hast}} \frac{(T_{\text{WI}+1} + T_{\text{WI}-1} - 2T_{\text{WI}})}{(\Delta x)^2} \quad (\text{A13})$$

where the subscripts on  $T$  refer to the increments along the test panel in the axial direction. The wall temperature  $T_{\text{W}}$  used for this calculation is the arithmetic average of  $T_{\text{WC}}$  and  $T_{\text{WA}}$ .

The film air temperature was determined by using the techniques given in reference 11:

$$f = \frac{T_{\text{H}} - T_{\text{f}}}{T_{\text{H}} - T_{\text{an}}} = \frac{1}{1 + C_{\text{m}} \frac{x}{M_{\text{s}}}} \quad (\text{A14})$$

The mass flux ratio is

$$M = \frac{\rho_{\text{s}} U_{\text{s}}}{\rho_{\text{H}} U_{\text{H}}} \quad (\text{A15})$$

For the combustor under investigation,  $C_{\text{m}} = 0.05$ .

The flame temperature input to the heat-transfer equations corresponds to the combustor exit temperature determined through exhaust gas analysis for the higher fuel-air ratios (0.04 and 0.05). At the lower fuel-air ratios (0.02 and 0.03), best results were obtained by using the adiabatic flame temperature for fuel-air ratios that were adjusted upward to account for the film-cooling air injected downstream of the instrumented panel. This resulted in input flame temperatures approximately 100 K greater than the exhaust gas temperatures. This adjustment was not necessary for the higher fuel-air ratios because the greater inefficiency of the flame at the axial location of the special panel kept the flame temperature down.

All these equations and inputs were used in an iterative computational technique to solve for liner wall temperature. Initially, equation (A1) was solved by neglecting axial conduction. This resulted in different wall temperatures at varying axial positions because of the change in film-cooling efficiency at incremental distances from the film-cooling slot. The wall temperatures resulting from this one-dimensional heat-transfer calculation were then used as the initial estimates in calculations that included the axial thermal conduction term. The solution technique then iterated on wall temperature until a convergence criterion of 0.3 degree Kelvin was met.

## APPENDIX B

### SYMBOLS

C	convective heat flux
$C_m$	turbulent mixing coefficient
D	hydraulic diameter
f	film air temperature
h	convective heat-transfer coefficient
K	thermal conductivity
KC	thermal conductive heat flux
M	mass flux ratio
Pr	Prandtl number
R	radiation heat flux
Re	Reynolds number
s	slot height
T	temperature
U	velocity
x	axial distance from film-slot exit
$\alpha$	absorptivity
$\delta$	thickness
$\epsilon$	emissivity
$\rho$	mass density
$\sigma$	Stefan-Boltzmann constant

#### Subscripts:

an	annulus conditions
c	casing
cerm	ceramic coating
eff	effective
f	gas film condition at any x
ft	flame tube

H	hot-gas conditions
Hast	Hastelloy
s	film-cooling slot conditions
W	liner wall
WA	liner wall - annulus side
WC	liner wall at ceramic metal interface
WH	liner wall - flame-tube side
WI	liner wall at increment I
1	flux to liner from flame-tube side
2	flux from liner to casing side

## REFERENCES

1. Stecura, Stephan; and Liebert, Curt H.: Thermal Barrier Coating System. U.S. Patent 4,055,705, Oct. 1977.
2. Liebert, Curt H.; and Stepka, Francis S.: Potential Use of Ceramic Coating as a Thermal Insulation on Cooled Turbine Hardware. NASA TM X-3352, 1976.
3. Liebert, Curt H.; et al.: Durability of Zirconia Thermal-Barrier Ceramic Coatings on Air-Cooled Turbine Blades in Cyclic Jet Engine Operation. NASA TM X-3410, 1976.
4. Stecura, Stephan: Two-Layer Thermal Barrier Coating for Turbine Airfoils - Furnace and Burner Rig Test Results. NASA TM X-3425, 1976.
5. Liebert, Curt H.; Stecura, Stephan; and Brown, Jack E.: Ceramic Thermal Barrier Coating. Ind. Res., vol. 18, no. 10, Oct. 1976, p. 22.
6. Butze, Helmut F.; and Liebert, Curt H.: Effect of Ceramic Coating of JT8D Combustor Liner on Maximum Liner Temperatures and Other Combustor Performance Parameters. NASA TM X-73581, 1976.
7. Adam, Paul W.; and Norris, James W.: Advanced Jet Engine Combustor Test Facility. NASA TN D-6030, 1970.
8. The Design and Performance Analysis of Gas Turbine Combustion Chambers. Vol. 1, Theory and Practice of Design. NREC-1082-1, Northern Research and Engineering Corp., 1964.
9. Tacina, Robert R.; and Marek, Cecil J.: Film Cooling in a Combustor Operating at Fuel-Rich Exit Conditions. NASA TN D-7513, 1974.
10. Liebert, Curt H.: Emittance and Absorptance of NASA Ceramic Thermal Barrier Coating System. NASA TP-1190, 1978.
11. Marek, Cecil J.: Effect of Pressure on Tangential-Injection Film Cooling in a Combustor Exhaust Stream. NASA TM X-2809, 1973.
12. Marek, Cecil J.; and Juhasz, Albert J.: Simultaneous Film and Convective Cooling of a Plate Inserted in the Exhaust Stream of a Gas Turbine Combustor. NASA TN D-7156, 1973.

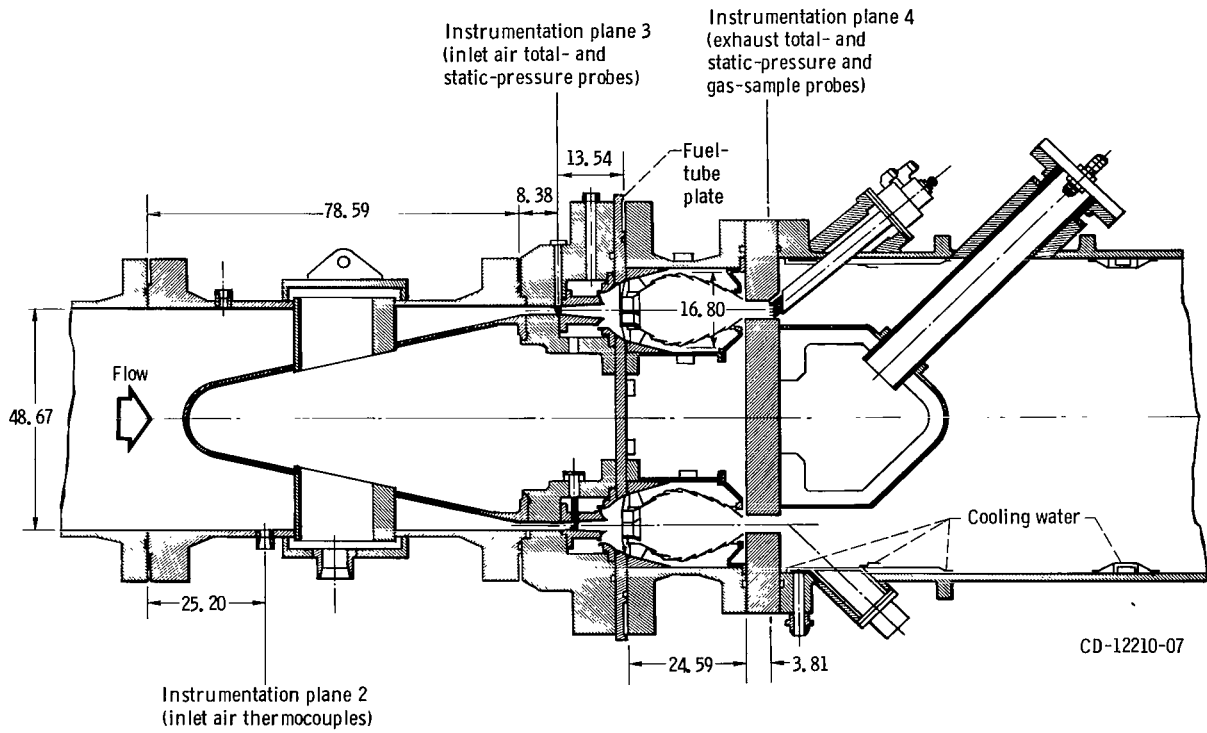
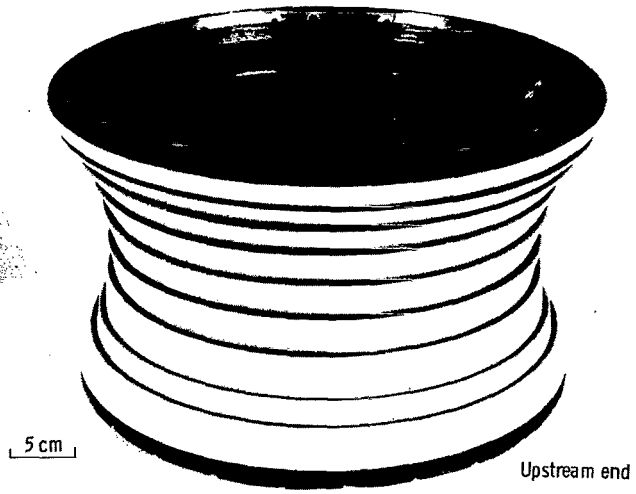
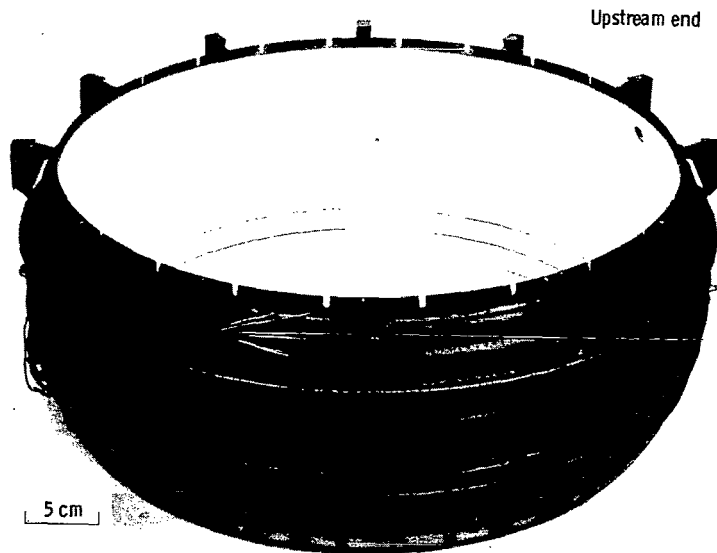


Figure 1. - Schematic cross section of combustion test rig showing combustor liner test section. (Dimensions are in centimeters.)



C-77-2732

(a) Inner diameter liner.



C-77-2733

(b) Outer diameter liner.

Figure 3. - Combustor liner with ceramic coating.

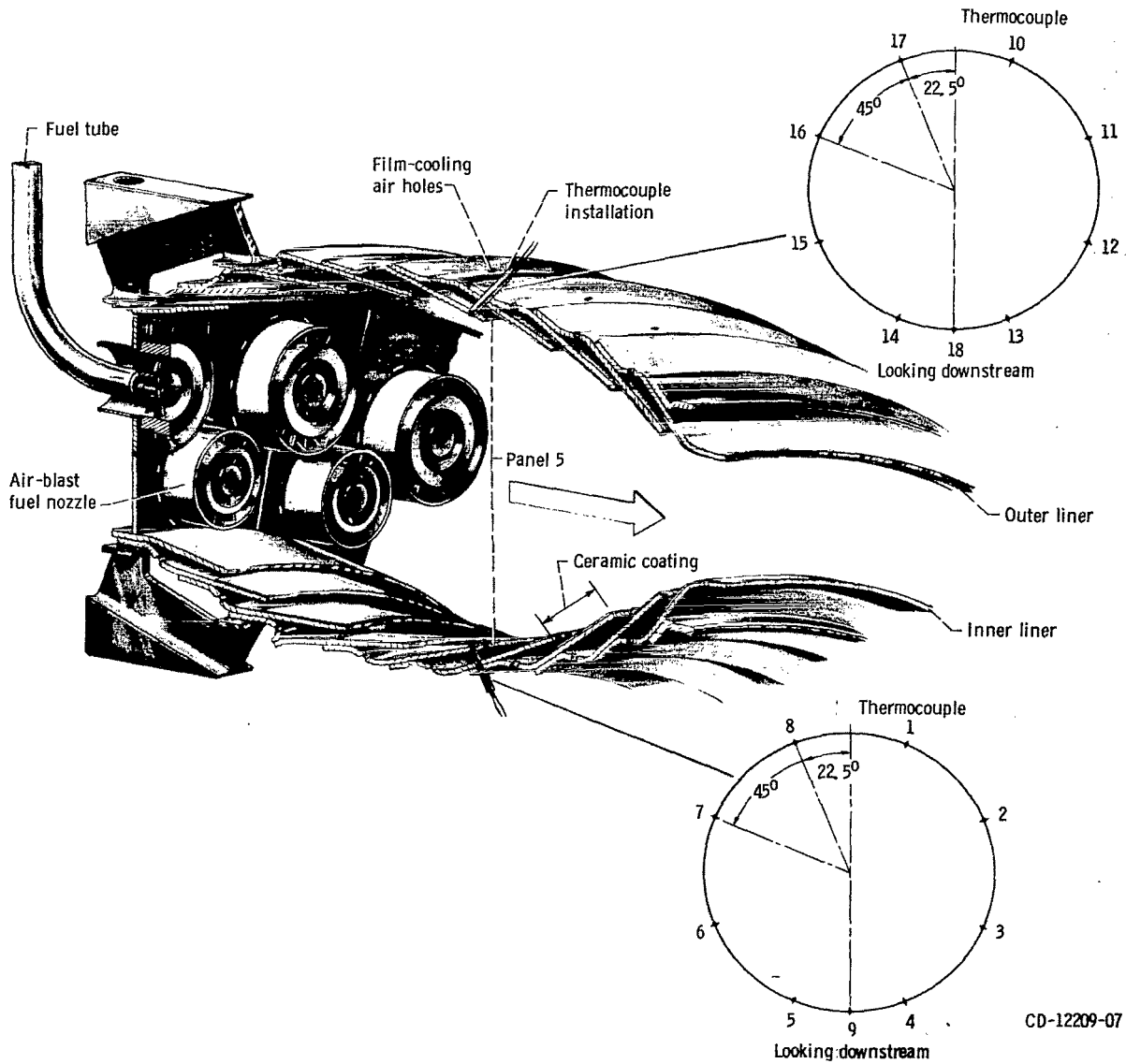
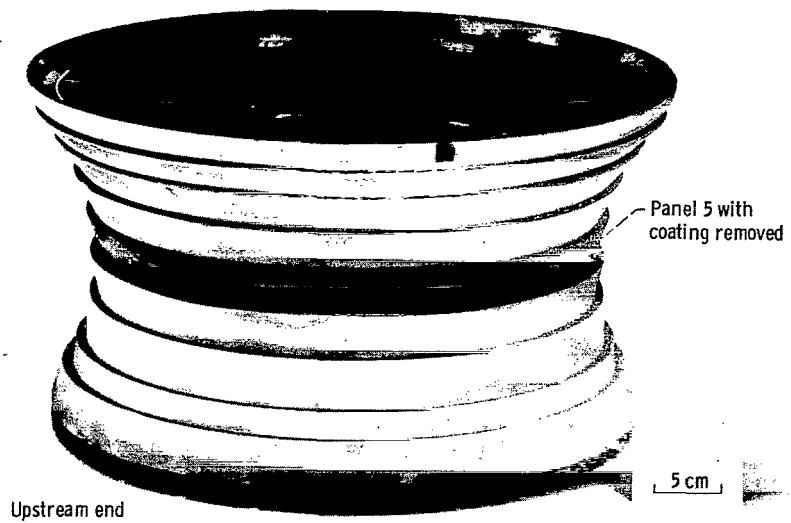
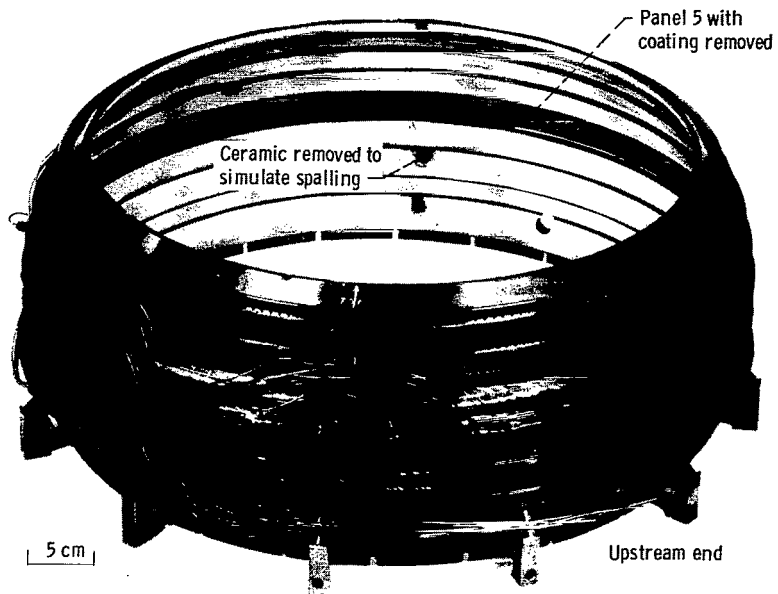


Figure 2 - Schematic illustration of combustor liner, air-blast fuel nozzles, and liner thermocouple location.



C-77-4780

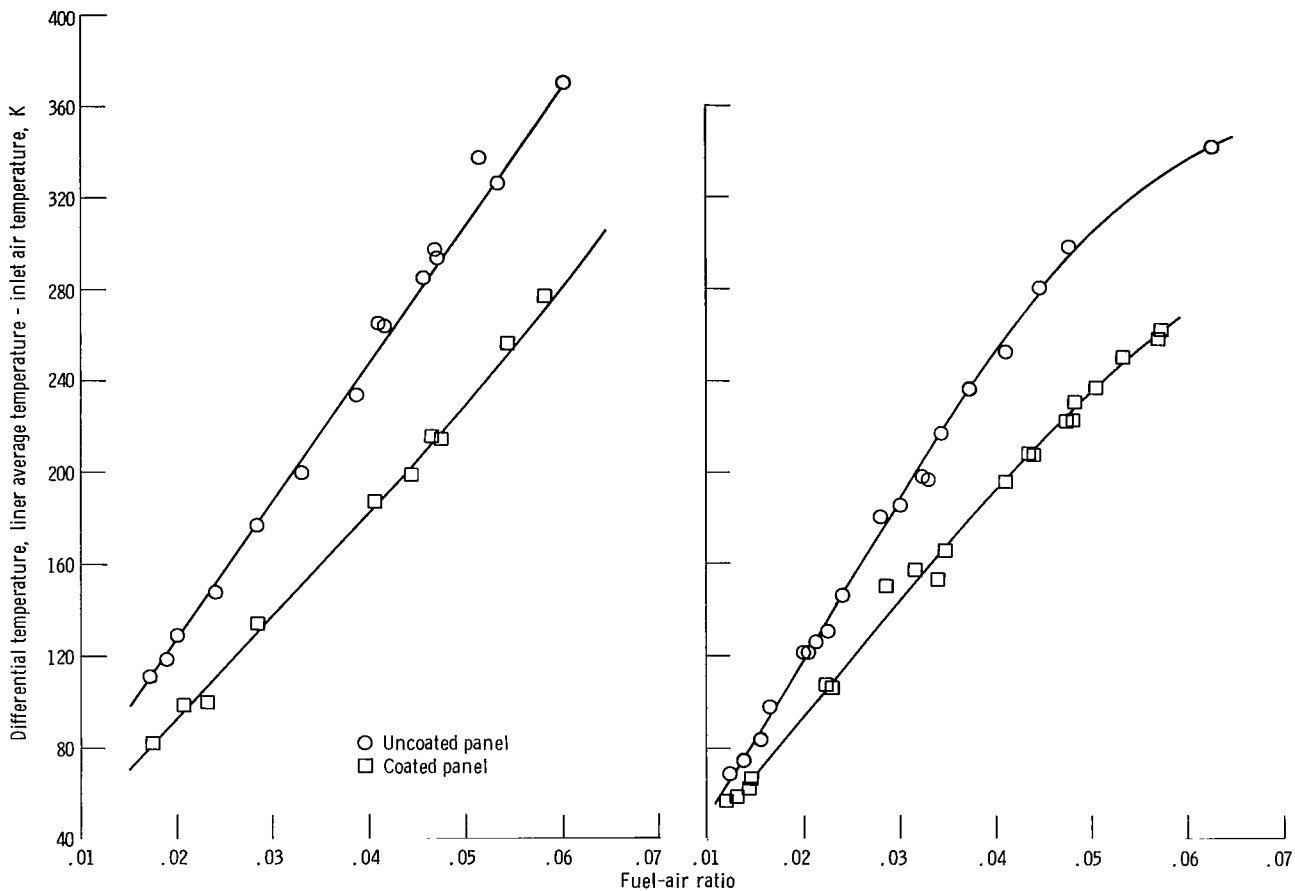
(a) Inner diameter liner.



C-77-4783

(b) Outer diameter liner.

Figure 4. - Combustor liner showing ceramic coating removed from panel 5.



(a) Nominal inlet air temperature, 589 K.

(b) Nominal inlet air temperature, 894 K.

Figure 5. - Effect of ceramic coating on combustor liner average metal temperature at various fuel-air ratios. Combustor inlet total pressure, 0.50 to 0.73 megapascal.

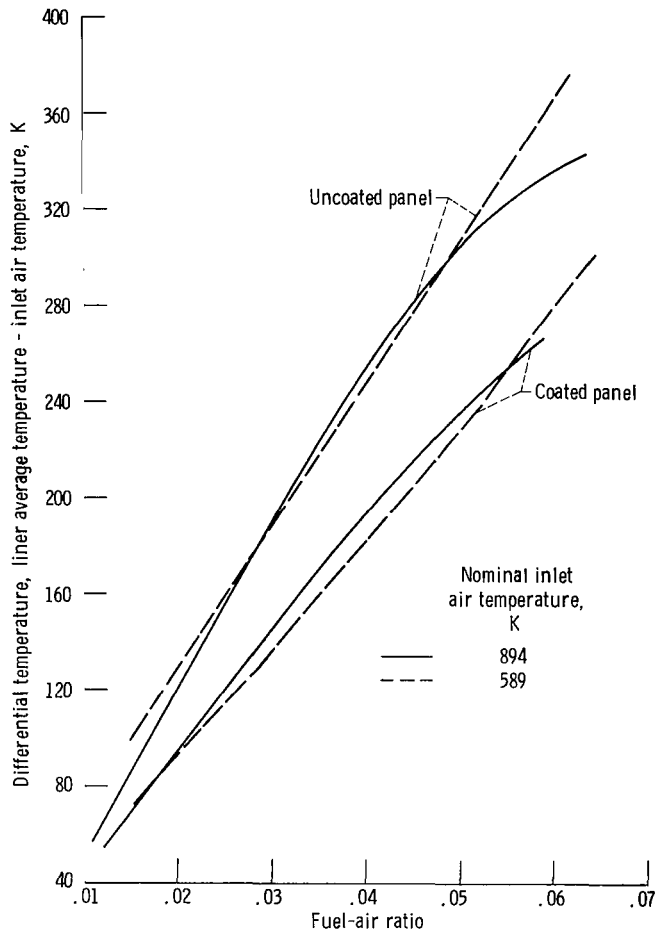


Figure 6. - Combustor liner metal temperatures with and without ceramic coating at two inlet air temperatures. Combustor inlet total pressure, 0.50 to 0.73 megapascal.

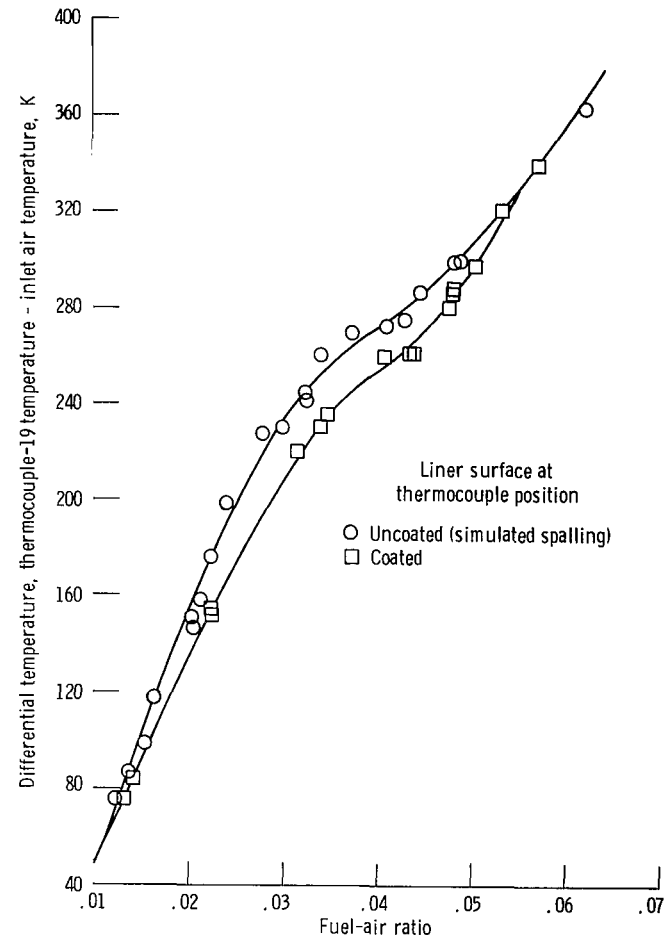
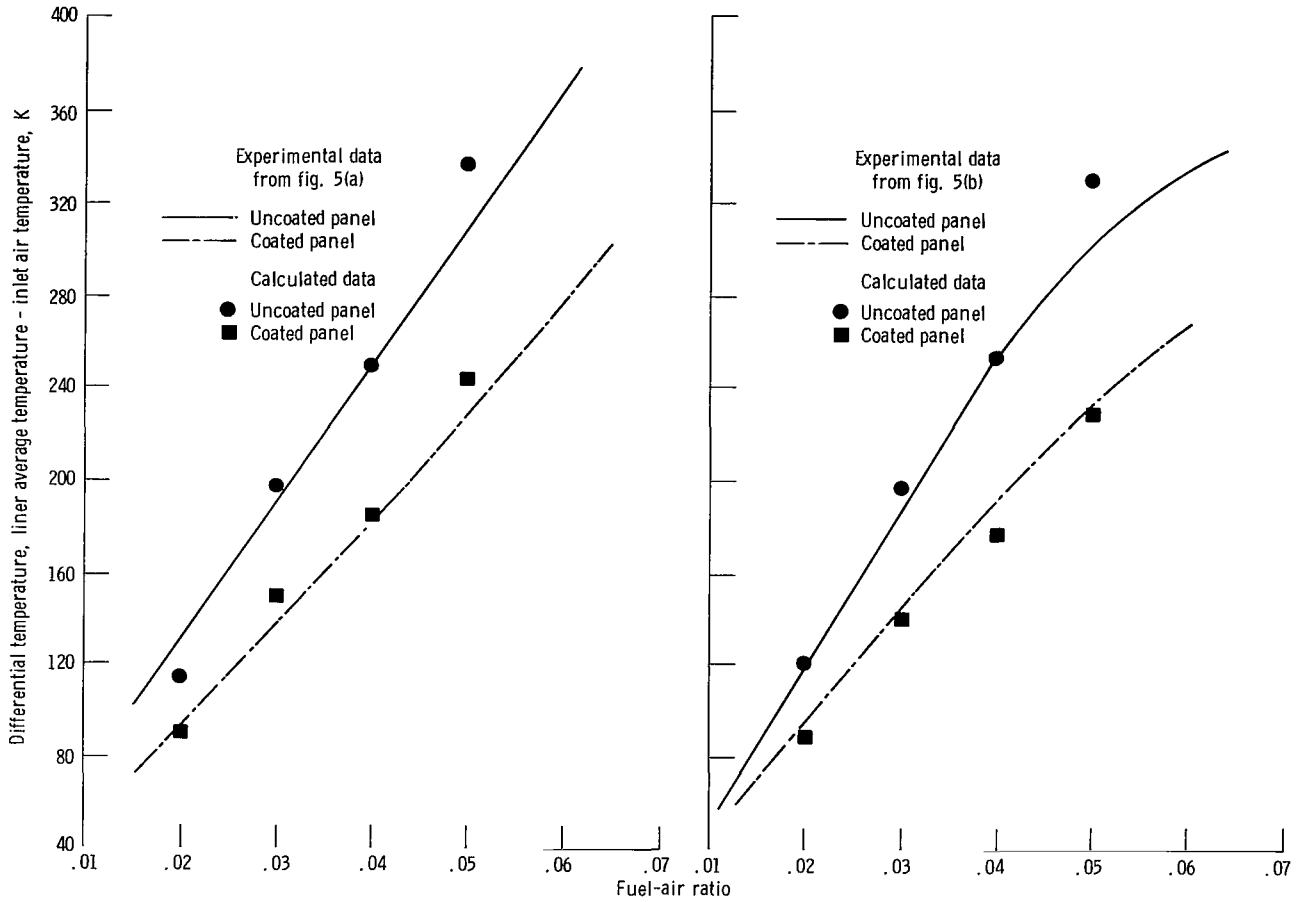


Figure 7. - Effect of simulated spalling of ceramic coating from combustor liner on liner metal temperature. Combustor inlet total pressure, 0.50 to 0.73 megapascal; nominal inlet air temperature, 894 K.



(a) Nominal inlet air temperature, 589 K.

(b) Nominal inlet air temperature, 894 K.

Figure 8. - Experimental and calculated combustor liner metal temperatures with and without ceramic coating at various fuel-air ratios. Combustor inlet total pressure, 0.50 to 0.73 megapascal.

1. Report No. <b>NASA TP-1323</b>	2. Government Accession No.	3. Recipient's Catalog No.	
4. Title and Subtitle <b>CERAMIC COATING EFFECT ON LINER METAL TEMPERATURES OF FILM-COOLED ANNULAR COMBUSTOR</b>		5. Report Date <b>January 1979</b>	6. Performing Organization Code
7. Author(s) <b>Russell W. Claus, Jerrold D. Wear, and Curt H. Liebert</b>		8. Performing Organization Report No. <b>E-9732</b>	10. Work Unit No. <b>505-04</b>
9. Performing Organization Name and Address <b>National Aeronautics and Space Administration Lewis Research Center Cleveland, Ohio 44135</b>		11. Contract or Grant No.	13. Type of Report and Period Covered <b>Technical Paper</b>
12. Sponsoring Agency Name and Address <b>National Aeronautics and Space Administration Washington, D. C. 20546</b>		14. Sponsoring Agency Code	
15. Supplementary Notes			
16. Abstract An experimental and analytical investigation was conducted to determine the effect of a ceramic coating on the average metal temperatures of a full-annular, film-cooled combustion chamber liner. This investigation was conducted at pressures from 0.50 to 0.73 MPa, inlet air temperatures of 589 and 894 K, and overall fuel-air ratios from 0.012 to 0.062. At all test conditions, experimental results indicate that application of a ceramic coating will result in significantly lower wall temperatures. In a simplified heat-transfer analysis, good agreement between experimental and calculated liner temperatures was achieved. Simulated spalling of a small portion of the ceramic coating resulted in only small increases in liner temperature because of the thermal conduction of heat from the hotter, uncoated area to the adjacent, coated liner metal.			
17. Key Words (Suggested by Author(s)) <b>Liner temperatures Ceramic coating</b>		18. Distribution Statement <b>Unclassified - unlimited STAR Category 07</b>	
19. Security Classif. (of this report) <b>Unclassified</b>	20. Security Classif. (of this page) <b>Unclassified</b>	21. No. of Pages <b>22</b>	22. Price* <b>A02</b>

\* For sale by the National Technical Information Service, Springfield, Virginia 22161

NASA-Langley, 1979

National Aeronautics and  
Space Administration

SPECIAL FOURTH CLASS MAIL  
BOOK

Postage and Fees Paid  
National Aeronautics and  
Space Administration  
NASA-451



Washington, D.C.  
20546

Official Business

Penalty for Private Use, \$300

5 1 10, A, 121878 S00903DS  
DEPT OF THE AIR FORCE  
AF WEAPONS LABORATORY  
ATTN: TECHNICAL LIBRARY (SUL)  
KIRTLAND AFB NM 87117

**NASA**

POSTMASTER: If Undeliverable (Section 158  
Postal Manual) Do Not Return

---